Differential Functional Connectivity along the Long Axis of the Hippocampus Aligns with Differential Role in Memory Specificity and Generalization

Lea E. Frank*, Caitlin R. Bowman*, and Dagmar Zeithamova

Abstract

■ The hippocampus contributes to both remembering specific events and generalization across events. Recent work suggests that information may be represented along the longitudinal axis of the hippocampus at varied levels of specificity: detailed representations in the posterior hippocampus and generalized representations in the anterior hippocampus. Similar distinctions are thought to exist within neocortex, with lateral prefrontal and lateral parietal regions supporting memory specificity and ventromedial prefrontal and lateral temporal cortices supporting generalized memory. Here, we tested whether functional connectivity of anterior and posterior hippocampus with cortical memory regions is consistent with these proposed dissociations. We predicted greater connectivity of anterior hippocampus with putative generalization regions and posterior hippocampus with putative memory specificity regions. Furthermore, we tested whether differences in connectivity are stable under varying levels of task engagement. Participants learned to categorize a set of stimuli outside the scanner, followed by an fMRI session that included a rest scan, passive viewing runs, and category generalization task runs. Analyses revealed stronger connectivity of ventromedial pFC to anterior hippocampus and of angular gyrus and inferior frontal gyrus to posterior hippocampus. These differences remained relatively stable across the three phases (rest, passive viewing, category generalization). Whole-brain analyses further revealed widespread cortical connectivity with both anterior and posterior hippocampus, with relatively little overlap. These results contribute to our understanding of functional organization along the long axis of the hippocampus and suggest that distinct hippocampal–cortical connections are one mechanism by which the hippocampus represents both individual experiences and generalized knowledge. ■

INTRODUCTION

Healthy memory function involves both the ability to remember details of individual events (specificity) and the ability to link related experiences to form new knowledge (generalization). It is well established that the hippocampus supports rapid learning of specific events (Vargha-Khadem et al., 1997; Bunsey & Eichenbaum, 1996; Scoville & Milner, 1957). More recent work has also demonstrated a role for the hippocampus in integrating related events to form generalized memories (Bowman & Zeithamova, 2018; Zeithamova, Dominick, & Preston, 2012; Shohamy & Wagner, 2008). How the hippocampus can simultaneously support memory for individual experiences and knowledge generalization is an area of active investigation (Berens & Bird, 2017; Schapiro, Turk-Browne, Botvinick, & Norman, 2017; Poppenk, Evensmoen, Moscovitch, & Nadel, 2013).

A recent proposal suggests that information is represented at varying levels of specificity along the long axis of the hippocampus: Representations in the posterior hippocampus are thought to be detailed and fine-grained, whereas those in the anterior hippocampus are more coarse and global (Poppenk et al., 2013). This hypothesis stems from animal research showing that receptive fields of hippocampal place cells increase in size from the dorsal (analogue of human posterior) to ventral (analogue of human anterior) hippocampus (Kjelstrup et al., 2008), representing information at increasingly larger spatial scales. Recent work has extended this representational gradient to humans, finding that fMRI signals within the anterior hippocampus were more correlated across voxels and self-correlated across time than signals in the posterior hippocampus (Brunec et al., 2018), consistent with the idea that posterior hippocampus represents events on a fine-grained temporal and spatial scale to capture detailed variations whereas anterior hippocampal representations span a larger temporal and spatial scale to enable generalization across events. Two recent fMRI findings further corroborate this idea. In an associative inference task where participants encoded overlapping pairs of items that shared a common element (A–B, B–C), Schlichting, Mumford, and Preston (2015) found that the anterior hippocampus formed integrated representations of the overlapping events (A–B–C representation), whereas overlapping event representations remained separated in the

University of Oregon
*These authors contributed equally to this work.

posterior hippocampus. Collin, Milivojevic, and Doeller (2015) found hierarchical representations of narratives along the hippocampal long axis, from individual events to multievent narratives, suggesting that this functional organization may be a consistent property of the hippocampus that spans multiple domains.

In addition to functional differences within the hippocampus, regions outside the hippocampus also differentially contribute to memory specificity and generalization. Lateral pFC, particularly the inferior frontal gyrus (IFG), supports memory specificity by resolving interference between related items (Bowman & Dennis, 2016; Kuhl, Dudukovic, Kahn, & Wagner, 2007; Badre & Wagner, 2005; Jonides, Smith, Marshuetz, Koeppe, & Reuter-Lorenz, 1998). Additionally, portions of posterior parietal cortex such as the angular gyrus (ANG) support memory specificity by representing individual items with high fidelity during retrieval (Xiao et al., 2017; Kuhl & Chun, 2014). Distinct regions have been implicated in memory generalization. The ventromedial pFC (VMPFC) contributes to generalization by integrating related memories during encoding (Schlichting et al., 2015; Zeithamova et al., 2012), encoding new information in light of prior knowledge (van Kesteren et al., 2013), and transferring conceptual knowledge to new examples (Bowman & Zeithamova, 2018; Kumaran, Summerfield, Hassabis, & Maguire, 2009). Lateral temporal cortices, especially the middle temporal gyrus (MTG), also support generalized memories, such as semantic memory (Mummery et al., 2000), conceptual knowledge (Bowman & Zeithamova, 2018; Davis & Poldrack, 2014), and "gist" representations (Turney & Dennis, 2017; Dennis, Kim, & Cabeza, 2008).

Despite evidence that generalized and specific memory representations exist both within the hippocampus and in cortex, we know relatively little about how regions supporting these distinct functions interact with one another. Studies have shown strong functional connections during rest between the hippocampus (as a whole) and the cortical regions indicated above, including the medial pFC, lateral temporal cortices, and portions of parietal cortex (Andrews-Hanna, Reidler, Sepulcre, Poulin, & Buckner, 2010; Vincent et al., 2006). However, evidence is mixed regarding functional connectivity differences along the long axis of the hippocampus (Blessing, Beissner, Schumann, Brünner, & Bär, 2016; Robinson, Salibi, & Deshpande, 2016; Wang, Ritchey, Libby, & Ranganath, 2016). Recent studies have also started to investigate the functional relevance of hippocampal–cortical connectivity for memory specificity and generalization. Regarding specificity, hippocampal–IFG connectivity supports subtle memory discriminations during retrieval (Bowman & Dennis, 2016; Manelis, Paynter, Wheeler, & Reder, 2013), and neural stimulation manipulating the strength of hippocampal–parietal connectivity can lead to enhancement of associative memory (Tambini, Nee, & D'Esposito, 2017; Wang et al., 2014). Regarding generalization, studies have focused on hippocampal–VMPFC connectivity, which has been shown to track the demands on memory integration during encoding (Zeithamova et al., 2012; van Kesteren, Fernandez, Norris, & Hermans, 2010). Furthermore, individual differences in hippocampal–VMPFC connectivity track individual differences in generalization performance (Gerraty, Davidow, Wimmer, Kahn, & Shohamy, 2014; van Kesteren et al., 2010), with "smaller" connectivity values associated with better performance. Recent work has also linked portions of lateral temporal cortices to this hippocampal–VMPFC circuit (Liu, Grady, & Moscovitch, 2017, 2018), but not in a memory generalization task, leaving the role of this region in generalization unclear.

In this study, we sought to characterize differences in hippocampal–cortical connectivity along the long axis of the hippocampus during rest and in the context of a generalization task. Participants first trained outside the scanner to classify cartoon animals into two novel categories and then completed three types of tasks while undergoing fMRI: rest, passive viewing of training and generalization items, and active classification of training and generalization items. We hypothesized that putative memory specificity regions (IFG, ANG) would show stronger connectivity with posterior compared with anterior hippocampus, whereas putative generalization regions (VMPFC, MTG) would show stronger connectivity with anterior compared with posterior hippocampus. We further hypothesized that the strength of these functional connections, especially the connectivity between anterior hippocampus and cortical generalization regions, would be related to generalization performance.

To measure connectivity across all task stages, we focused primarily on background connectivity, a functional connectivity measure of low-frequency signal coupling between regions after trial-by-trial signal fluctuations are removed. One view of background connectivity emphasizes its dynamic nature, where background connectivity is interpreted to be reflective of temporary brain states associated with cognitive processes, such as levels of attention (Al-Aidroos, Said, & Turk-Browne, 2012), emotional arousal (Tambini, Rimmele, Phelps, & Davachi, 2017), encoding versus retrieval (Duncan, Tompary, & Davachi, 2014), and goal states (Norman-Haignere, McCarthy, Chun, & Turk-Browne, 2012). In contrast, other research has underscored that patterns of connectivity are relatively stable across levels of external task engagement (Frank, Preston, & Zeithamova, 2019; Horien, Shen, Scheinost, & Constable, 2019; Gratton et al., 2018; Touroutoglou, Andreano, Barrett, & Dickerson, 2015), with measures of background connectivity providing principally the same information as measures of resting-state connectivity. Thus, we computed both background connectivity across levels of task engagement and traditional resting-state connectivity to test whether any observed differences in anterior and posterior hippocampal connectivity with cortical memory regions are dynamic characteristics driven by task engagement or whether they reflect stable characteristics of hippocampal memory

networks. If the anticipated anterior and posterior connectivity differences are driven by generalization demands, we might expect them to emerge only when participants are actively categorizing items. If connectivity patterns are relatively stable, we can principally obtain the same information from whichever phase of the experiment (including rest alone), but including all phases provides us with the best estimates of connectivity values for each connection based on all available data.

METHODS

Participants

The sample size was determined based on an a priori power analysis conducted for the task-based analyses presented in Bowman and Zeithamova (2018), which determined a sample size of $n = 32$ to be adequate to detect category representations in hippocampus and VMPFC with 80% power. Based on the expected 15–20% exclusion rate due to motion or poor task performance, we decided to collect 40 full data sets. Two participants did not complete the full scan and were immediately replaced. Thus, a total of 42 individuals were recruited from the University of Oregon and the surrounding community and received financial compensation for their participation. Sixteen participants were excluded from analyses for failing to complete the task (two participants), below-chance performance at the end of training and/or in the categorization test (five participants), structural abnormality (one participant), and excessive movement (movement >2 mm within a run or insufficient data remaining following scrubbing as described in fMRI preprocessing; eight participants), leaving data from 26 participants reported in all analyses (17 women; age = 18–28 years, mean age = 20.8 years, *SD* age = 3.0 years). All participants provided written informed consent, were right-handed, had learned English before age 7 years, and were screened for MRI contraindications, neurological conditions, and medications known to affect brain function. All experimental procedures were approved by Research Compliance Services and the University of Oregon.

Procedure

Participants completed four experimental phases: category training (outside the scanner), a resting-state scan, passive viewing of category examples, and a categorization phase that required generalization of category knowledge to new stimuli (Figure 1). Results of a task-based activation analysis of the categorization fMRI data have been reported (Bowman & Zeithamova, 2018), including detailed descriptions of the stimuli, category structure, training, and generalization task procedures. Briefly, participants first performed five blocks of feedback-based category training outside the scanner. Shortly thereafter, participants entered the scanner and completed a single run of rest, lasting 5 min, during which participants viewed a fixation cross and kept their eyes open. During two runs of passive viewing, participants viewed training items as well as new items of the same typicality without making overt responses. Participants were told to pay attention to each stimulus because they might be tested on them later. During categorization runs, participants viewed training items as well as novel items at all levels of typicality and classified them into the two categories using button presses. In both passive viewing and categorization, each stimulus was presented for 5 sec, followed by a 7-sec intertrial interval. Anatomical images were collected following categorization runs. After the scan, participants completed a brief questionnaire and were verbally debriefed. Connectivity was measured during rest, passive viewing, and categorization.

fMRI Data Acquisition

Scanning was completed on a 3T Siemens MAGNETOM Skyra scanner equipped with a 32-channel head coil at the University of Oregon Lewis Center for Neuroimaging. Head motion was minimized using foam padding.

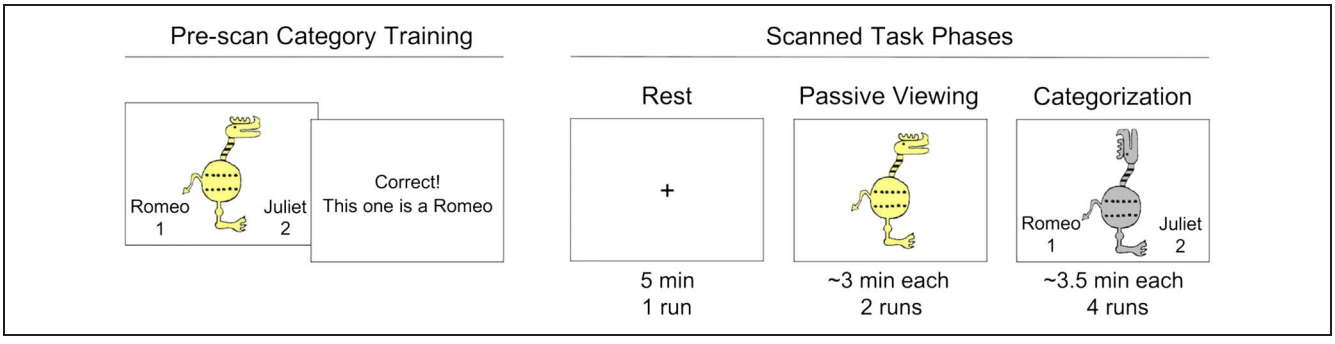

Figure 1. Behavioral procedures. Before the fMRI scan, participants were trained on the category structures of cartoon animals. The scanned portion of the task consisted of three phases that demanded varying levels of engagement. During rest, participants did not perform any task and were not required to give responses. During passive viewing, participants viewed old and new stimuli without giving any response. During categorization, participants viewed old and new stimuli while responding to which category each one belonged.

The scanning session started with a localizer scan followed by seven functional runs using a multiband gradient-echo pulse sequence (repetition time [TR] = 2000 msec, echo time [TE] = 26 msec, flip angle = 90°, matrix size = 100 × 100, 72 contiguous slices oriented 15° off the anterior commissure–posterior commissure line to reduce prefrontal signal dropout, interleaved acquisition, field of view [FOV] = 200 mm, voxel size = 2.0 × 2.0 × 2.0 mm, generalized autocalibrating partially parallel acquisitions [GRAPPA] factor = 2). One hundred fifty volumes were collected for the rest scan, 100 volumes were collected for each passive viewing run, and 106 volumes were collected for each categorization run. A standard high-resolution T1-weighted MPRAGE anatomical image (TR = 2500 msec, TE = 3.43 msec, inversion time = 1100 msec, flip angle = 7°, matrix size = 256 × 256, 176 contiguous slices, FOV = 256 mm, slice thickness = 1 mm, voxel size = 1.0 × 1.0 × 1.0 mm, GRAPPA factor = 2) was collected following all functional runs. Scanning concluded with a custom anatomical T2 coronal image (TR = 13,520 msec, TE = 88 msec, flip angle = 150°, matrix size = 512 × 512, 65 contiguous slices oriented perpendicularly to the main axis of the hippocampus, interleaved acquisition, FOV = 220 mm, voxel size = 0.4 × 0.4 × 2 mm, GRAPPA factor = 2).

ROIs

ROIs were defined anatomically in individual participants' native space based on the cortical parcellations and subcortical segmentation from Freesurfer Version 6 (https://sufer.nmr.mgh.harvard.edu/) and collapsed across hemispheres (Figure 2). We defined anterior and posterior hippocampal ROIs separately for each participant by dividing the Freesurfer hippocampal ROI at the middle slice. If there were an odd number of slices, the middle slice was assigned to the posterior hippocampus. We chose the IFG, ANG, VMPFC, and MTG for our cortical ROIs based on their differential involvement in memory generalization and specificity. The IFG ROI was obtained by combining the three IFG subregions (labeled as pars opercularis, pars orbitalis, and pars triangularis) provided by Freesurfer. The ANG ROI was defined using the 2009 Freesurfer parcellations inferior parietal-angular part label (Destrieux, Fischl, Dale, & Halgren, 2010). The VMPFC ROI consisted of Freesurfer-defined medial OFC. The MTG ROI was defined using the Freesurfer MTG label. All individual participant anatomical ROIs were resampled to functional space using ANTs (Advanced Normalization Tools; stnava.github.io/ANTs/) and applied as masks to extract the mean time series from each region.

fMRI Preprocessing

Raw dicom images were converted to Nifti format using the *dcm2nii* function from MRIcron (https://www.nitrc.org/projects/mricron). Functional images were skull stripped using BET (brain extraction tool), which is part of FSL Version 5.0.9 (www.fmrib.ox.ac.uk/fsl). Motion correction was computed within each functional run using MCFLIRT in FSL to realign all volumes to the middle volume. Across-run realignment was computed using ANTs with the first functional volume serving as the reference volume. The first volumes of all other runs were registered to the reference volume, and the transformation computed was applied to all other images in the run. Brain-extracted and motion-corrected images from each rest, passive viewing, and categorization run were entered into the FEAT (fMRI Expert Analysis Tool) in FSL for high-pass temporal filtering (100 sec) and spatial smoothing using a 2-mm FWHM kernel.

As connectivity measures can be inflated by motion and physiological noise, additional steps are required to control for these confounds when calculating connectivity (Murphy, Birn, & Bandettini, 2013; Power, Barnes, Snyder, Schlaggar, & Petersen, 2012). First, we extracted the time series for cerebrospinal fluid, white matter, and whole-brain signal and calculated framewise displacement (FD) and global signal change (DVARS) for each functional scan. These values were used as nuisance regressors when calculating connectivity (see below) and used to determine individual volumes for exclusion. Individual volumes were flagged for exclusion if either FD exceeded 0.5 mm or DVARS exceeded 0.5%, as well as one volume before and two volumes after each flagged volume (Power et al., 2012). The first two volumes of each run were also excluded. This scrubbing procedure flagged for removal an average of 6.9% of volumes from

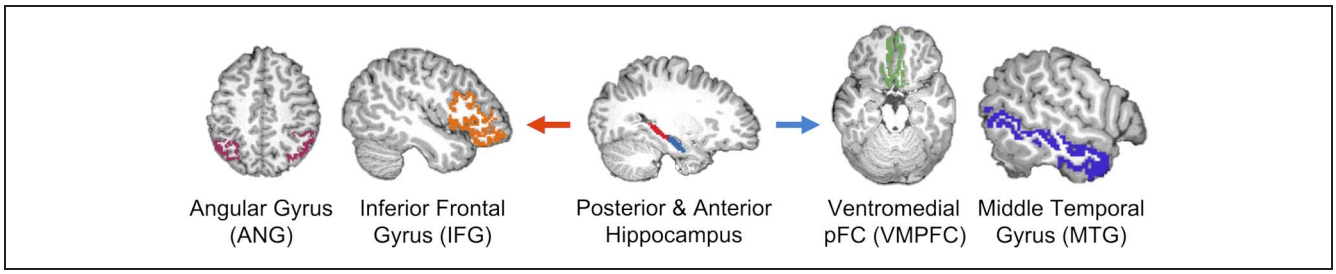

Figure 2. ROIs. Functional connectivity was measured between posterior (red) and anterior (blue) hippocampus with each of the four cortical ROIs. We predicted that posterior hippocampus would be preferentially connected to ANG and IFG, whereas anterior hippocampus would show greater connectivity with VMPFC and MTG.

rest, an average of 5.3% from passive viewing runs, and an average of 6.8% from categorization runs. Individual runs were excluded from analyses if over 30% of volumes were flagged for removal. All participants included in the final analyses had the rest run and both passive viewing runs. For three participants, one or two categorization runs were excluded from the final analysis. Participants were excluded entirely if they had more than two individual runs excluded across all functional runs (two participants).

Measuring Connectivity

When measuring background connectivity, the aim is to remove the effect of coactivation driven by external stimuli before calculating connectivity. For example, if two regions respond to the same stimulus, their signal will increase synchronously whenever a stimulus is presented, irrespective of whether these regions communicate with each other. One method for removing task-related signal from the time series is to first model task-related activation and compute connectivity on the residuals. However, as the actual hemodynamic response to each stimulus likely differs somewhat from the model, some residual task-related activation likely remains. A more recent approach for removing task-related signals is to use a low-pass filter set below the task frequency (e.g., Tambini, Rimmele, et al., 2017; Norman-Haignere et al., 2012). Although it is impossible to rule out that some low-frequency task-related features remain, this method can successfully remove trial-by-trial signal fluctuations that may otherwise drive connectivity measures.

Adopting this approach here, all functional scans, including rest, were filtered with a Gaussian linear low-pass filter (16 sec) to remove activity cycling faster than task frequency (12 sec during both passive viewing and categorization). To determine the appropriate threshold for the low-pass filter, we examined the power spectrum of the BOLD signal from the lateral occipital cortex during a single categorization run (see Figure 3 for an example participant). A conservative threshold of 16 sec was chosen to adequately remove task-related frequencies. Although low-pass filtering is not commonly applied to rest scans, it was necessary to apply it here for analyses that compare connectivity during rest scans with background connectivity measured during task-based scans (Frank et al., 2019; Van Dijk et al., 2010). We also recalculated all main analyses on rest connectivity only, using resting-state connectivity measures from non-low-pass filtered time series, to validate that our findings were not driven by additional preprocessing.

Following low-pass filtering (or no filtering), we excluded all the volumes previously flagged for exclusion before calculating connectivity. Connectivity was measured as the partial correlation between each hippocampal ROI (anterior and posterior hippocampus) and each cortical ROI (ANG, IFG, VMPFC, MTG) while controlling for motion and physiological noise. We included the standard six realignment motion parameters, the above-described physiological noise parameters (cerebrospinal fluid, white matter, whole brain signal), and all their derivatives as nuisance regressors. Excluded volumes were removed from all regressors. The resulting correlation coefficients were Fisher z-transformed for subsequent analysis.

Comparing Hippocampal Connectivity

To test whether functional connectivity differed between anterior and posterior hippocampus and if these differences depended on the task phase, we conducted a 2 (Hippocampal ROI: anterior, posterior) × 4 (Cortical ROI: ANG, IFG, VMPFC, MTG) × 3 (Phase: rest, passive viewing, categorization) repeated-measures ANOVA. Of particular interest was the interaction between Hippocampal ROI and Cortical ROI. Follow-up t tests were conducted to compare connectivity between anterior and posterior hippocampus with each cortical ROI. We predicted that memory specificity regions (ANG, IFG) would show greater connectivity with posterior than anterior hippocampus, whereas generalization regions (VMPFC, MTG) would be more connected to anterior than posterior hippocampus. The three-way interaction between

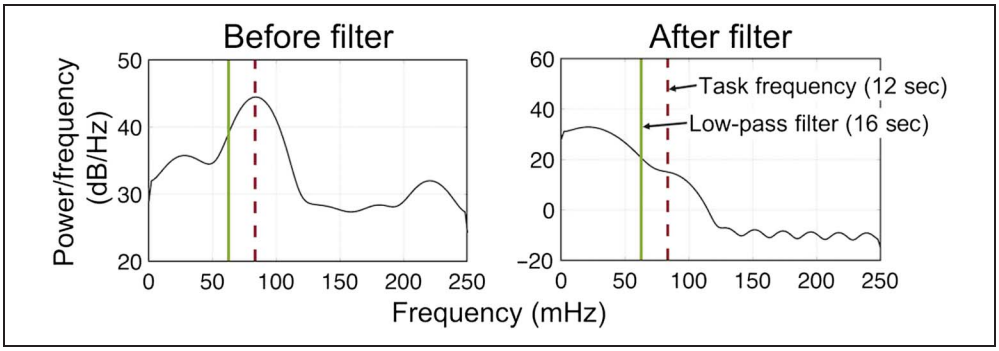

Figure 3. Low-pass filter for measuring background connectivity. Left: Power spectrum of a lateral occipital cortex signal during the first run of categorization for an example participant before filtering shows a peak at task frequency (dashed line, 83 mHz = 12 sec). A conservative threshold of 62.5 mHz = 16 sec (solid line) was chosen for the low-pass filter to assure the removal of all task-related frequencies, as demonstrated by a disappearance of the peak at task frequency on the right panel.

Hippocampal ROI, Cortical ROI, and Task phase was also examined to determine whether anterior and posterior hippocampal connectivity differences depended on the level of task engagement. The main effects of Hippocampal and Cortical ROIs were not interpreted as they were not of interest. The full results are reported in an ANOVA summary table.

Connectivity–Behavior Correlations

Although our sample size was chosen for task-based analyses and was small for an individual differences analysis, we wanted to replicate prior reports (Gerraty et al., 2014; van Kesteren et al., 2010) and test whether connectivity measures tracked behavioral generalization performance. We conducted a multiple regression with hippocampal–cortical connections as predictors and generalization (categorization accuracy for new stimuli) as the outcome. As these analyses were underpowered, the likelihood of Type II error was quite high, and the results should be interpreted with caution. To limit the number of predictors in a single model, separate regressions were conducted for anterior hippocampus connections and posterior hippocampus connections. We hypothesized that anterior hippocampus connectivity with generalization regions would be correlated with generalization success. In addition to average connectivity values, we also related behavior to connectivity within each phase separately to test the stability of connectivity–behavior relationships across phases. When a connection was a significant predictor of behavior in at least one phase, we then compared connection–behavior relationships across phases by computing a z test for equality of two dependent correlations (Steiger, 1980).

Continuous Hippocampal Connectivity

In addition to the dichotomous anterior versus posterior analysis, we were interested in whether connectivity differences along the hippocampal long axis were graded in nature. To test for a functional connectivity gradient, we measured connectivity continuously (i.e., in each slice) from the posterior to anterior hippocampus. The time series were extracted from each slice along the longitudinal axis of the hippocampal ROI in functional space individually for the right and left hippocampus in each participant. Peripheral slices that contained fewer than 15 voxels were excluded from the analysis. The number of voxels in slices retained for analyses ranged between 16 and 71 voxels, with a mean number of voxels = 32.49. Following the same procedures outlined above, connectivity was measured between each hippocampal slice in an individual participant and each ipsilateral cortical ROI. Because the length of the hippocampus differs between hemispheres and between individuals, the connectivity values from individual slices were interpolated using a weighted average into six bins (Brunec et al., 2018), resulting in six connectivity values for each hippocampal ROI, which were then averaged across hemispheres. Because task phase did not interact with anterior and posterior hippocampal connectivity differences in the prior ANOVA (see Results below), connectivity was averaged across the task phases and submitted to a 4 (Cortical ROI: ANG, IFG, VMPFC, and MTG) × 6 (Connectivity bin: posterior to anterior) repeated-measures ANOVA. Of particular interest was the interaction between Cortical ROI and Connectivity bin. Following a significant interaction (see Results), one-way ANOVAs were conducted to investigate the linear and quadratic effects of connectivity bin for each cortical ROI. Because hippocampal bins were numbered from posterior to anterior, a linear increase in connectivity across the six bins indicated increasing connectivity strength from posterior to anterior, whereas a linear decrease indicated increasing connectivity strength from anterior to posterior. We also examined quadratic effects of hippocampal bin to determine if connectivity was nonlinear along the posterior to anterior axis. For all ANOVAs reported in the paper, Greenhouse–Geisser corrections for sphericity were used when appropriate, indicated by "GG" in the resulting ANOVA reports.

Whole-brain Connectivity

Although our cortical ROIs were selected based on their contributions to different memory functions, we wanted to further characterize anterior and posterior hippocampus connectivity networks and their overlap across the whole brain. A general linear model was used to identify whole-brain correlations with two seed regions, the bilateral anterior hippocampus and bilateral posterior hippocampus, during each scanning phase. The mean time series for each anterior and posterior hippocampus ROI were entered as regressors into FSL FEAT, along with nuisance regressors (cerebrospinal fluid, white matter, whole brain signals, six motion parameters) and their derivatives. We first computed whole-brain connectivity separately for each participant and for each functional scan (one rest scan, two passive viewing scans, four categorization scans) using first-level analyses in FEAT. We then averaged the resulting connectivity maps across separate runs of the same task (passive viewing or categorization) in individual participants using fixed-effects higher level analyses in FEAT. We then generated a single whole-brain connectivity map per participant by averaging across the three scanning phases. These maps were normalized to MNI space and submitted to group-level analyses using one-sample t tests to identify regions showing connectivity with anterior and posterior hippocampus across the group. The resulting maps were thresholded using a voxel-wise threshold of $Z = 3.1$ and cluster-extent threshold of $p = .05$. As the whole-brain connectivity maps for both anterior and posterior hippocampus yielded, among others, a large cluster that

Table 1. Omnibus Connectivity ANOVA

Source	df_{effect}	df_{error}	F	p	η_p^2
Hippocampal ROI	1.00	25.00	0.27	.605	.01
Cortical ROI	3.00	75.00	22.95	.000	.48
Phase (GG)	1.58	39.57	0.41	.620	.02
Hippocampal ROI × Cortical ROI (GG)	2.20	54.98	24.95	.000	.50
Hippocampal ROI × Phase (GG)	1.99	49.69	0.90	.413	.04
Cortical ROI × Phase (GG)	3.93	98.12	2.96	.024	.11
Hippocampal ROI × Cortical ROI × Phase (GG)	4.28	106.93	1.53	.196	.06

spanned across many regions and three or four lobes, we further masked the statistical maps with anatomical masks for each lobe generated using the MNI Structural Atlas and reported significant clusters within each lobe. Multiple local maxima are reported when the resulting clusters spanned across multiple regions within a lobe. The masking procedure was only done to generate meaningful activation tables; the original activation maps are displayed in figures. Finally, we computed an overlap map using a conjunction of the anterior and posterior hippocampal connectivity maps, obtaining regions that were significantly connected with both anterior and posterior hippocampus.

RESULTS

Anterior versus Posterior Connectivity with Cortical Memory ROIs

To test whether cortical memory ROIs were differentially connected to anterior and posterior hippocampus and whether their connection strengths were modulated by task demands, we conducted a 2 (Hippocampal ROI: anterior, posterior) × 4 (Cortical ROI: ANG, IFG, VMPFC, MTG) × 3 (Phase: rest, passive viewing, categorization) repeated-measures ANOVA. The complete results of the ANOVA are reported in Table 1. Consistent with our prediction of differential connectivity patterns between anterior and posterior hippocampus, we found a significant interaction between Hippocampal ROI and Cortical ROI (Figure 4A). Follow-up t tests revealed that ANG, $t(25) = 3.82$, $p = .001$, $\eta_p^2 = .37$, and IFG, $t(25) = 2.07$, $p = .049$, $\eta_p^2 = .15$, showed greater connectivity with the posterior relative to anterior hippocampus, whereas VMPFC, $t(25) = 5.34$, $p < .001$, $\eta_p^2 = .53$, showed greater connectivity with anterior than posterior hippocampus. The MTG showed no significant difference in connectivity with anterior and posterior hippocampus, $t(25) = 0.66$, $p = .517$, $\eta_p^2 = .02$.

The overall pattern of connectivity was similar when measured using rest-only data without low-pass filtering. There was a significant interaction between Hippocampal and Cortical ROIs, $F(2.22, 55.39) = 25.37$, $p < .001$, $\eta_p^2 = .50$, GG, driven by greater VMPFC connectivity with anterior hippocampus, $t(25) = 6.99$, $p < .001$, $\eta_p^2 = .66$, and marginally greater ANG connectivity with posterior hippocampus, $t(25) = 1.93$, $p = .066$, $\eta_p^2 = .13$. IFG and MTG connectivity differences were numerically in the predicted direction but were not significant: IFG, $t(25) = 1.37$, $p = .184$, $\eta_p^2 = .07$; MTG, $t(25) = 0.30$, $p = .766$, $\eta_p^2 = .004$.

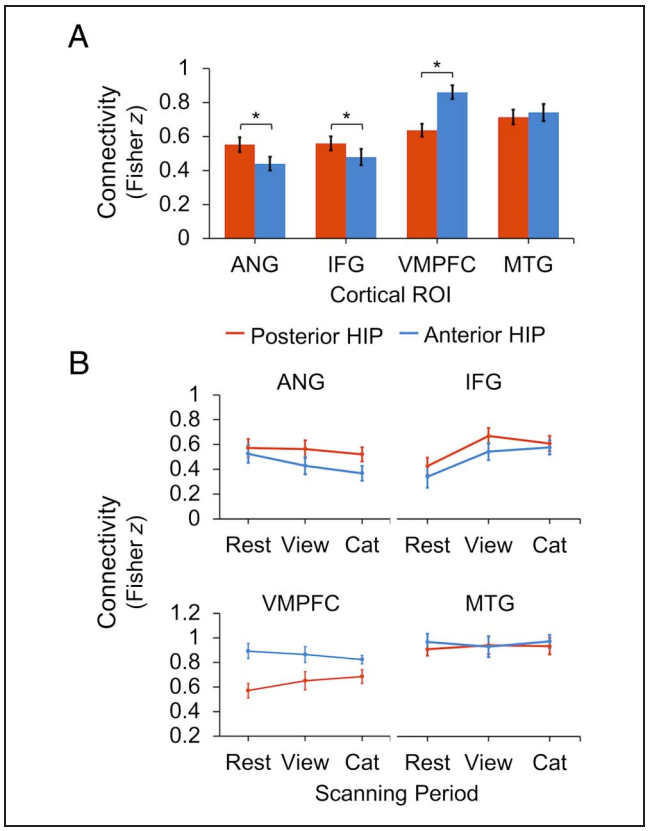

Figure 4. Anterior versus posterior hippocampal connectivity. (A) Low-frequency connectivity between anterior/posterior hippocampus and each cortical region, collapsed across phases. (B) Results of omnibus ANOVA examining connectivity between each hippocampal section (anterior, posterior) and each cortical ROI (ANG, IFG, VMPFC, MTG) in each task phase (rest, passive viewing, categorization).

The three-way interaction between Hippocampal ROI, Cortical ROI, and Task phase was not significant, suggesting that the anterior versus posterior differences in hippocampal connectivity were relatively stable across the task (Figure 4B). Although there was no significant three-way interaction, we did find a two-way interaction between Cortical ROI and Task phase. Follow-up one-way ANOVAs examined connectivity of each cortical ROI with the entire hippocampus (averaged across anterior and posterior) across the three task phases. The IFG was the only cortical region that demonstrated a significant effect of phase, $F(2, 50) = 4.90$, $p = .011$, $\eta_p^2 = .16$ (all others $F < 1$, $p > .4$). The effect of task phase in IFG was driven by significantly smaller IFG connectivity with the hippocampus during rest compared with passive viewing, $t(25) = 2.53$, $p = .018$, and categorization, $t(25) = 2.36$, $p = .026$, with no difference between passive viewing and categorization, $t(25) = 0.24$, $p = .813$. This finding suggests that low-frequency interactions between the IFG and hippocampus may be driven by task engagement, whereas interactions between the hippocampus and other cortical regions (ANG, VMPFC, MTG) are more stable.

Connectivity–Behavior Relationships

We tested whether the strength of hippocampal–cortical connectivity, averaged across phases, was related to participants' generalization performance using multiple regressions. Within the anterior hippocampal connections, we found VMPFC–anterior hippocampus connectivity to significantly predict categorization, $\beta = -.625$, $t(21) = -2.64$, $p = .015$. No other anterior hippocampal connection tracked performance (all $|\beta| < .37$, $|t(21)| < 1$, $p > .3$). However, given the small sample size for individual differences and the possibility of Type II error, the lack of a relationship to behavior in other ROIs should not be over interpreted. Within the posterior hippocampal connections, we found no connection to be a significant predictor of performance, but VMPFC–posterior hippocampus connectivity was a marginal predictor, $\beta = -.472$, $t(21) = -2.05$, $p = .053$ (all other connections $|\beta| < .32$, $|t(21)| < 1, p > .3$). Contrary to our prediction, the strength of the VMPFC connectivity–behavior relationship did not differ significantly between anterior and posterior hippocampus ($z = 0.17$, $p = .865$).

Given the negative direction of the connectivity–behavior relationship, we wanted to ensure that it was not driven by noncompliant participants performing poorly and having high connectivity values due to motion. We first tested whether motion (indexed by mean FD for each participant) can be predicted from connectivity values, computing the same regression as above but replacing generalization with mean FD as the dependent variable. No connection was found to significantly predict motion. Second, we recomputed the above regression with generalization as the outcome variable but included mean FD for each participant as a covariate. VMPFC–hippocampal connectivity remained a significant (anterior) and marginal (posterior) predictor of performance even after controlling for participants' motion.

Although the anterior versus posterior connectivity differences were relatively stable across task phases, we wanted to evaluate whether the connectivity–behavior relationship was relatively stable as well. We thus conducted the same

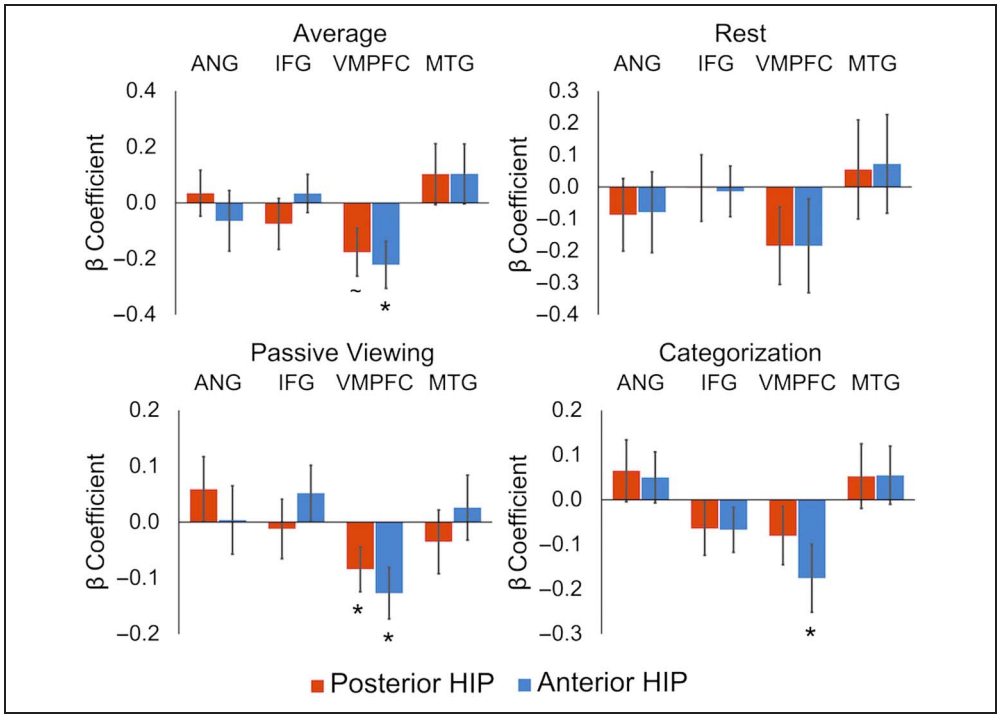

Figure 5. Connectivity–generalization relationships. Regressions were conducted on generalization performance using anterior hippocampal connections and posterior hippocampal connections as predictors. Separate models were then run at each task phase to test the relative stability of connectivity–behavior relationships. The rest phase connectivity values were derived from non-low-pass filtered time series for this figure for a more direct comparison to prior rest-based connectivity work, but analyses of low-pass filtered data also did not reveal any significant predictors.

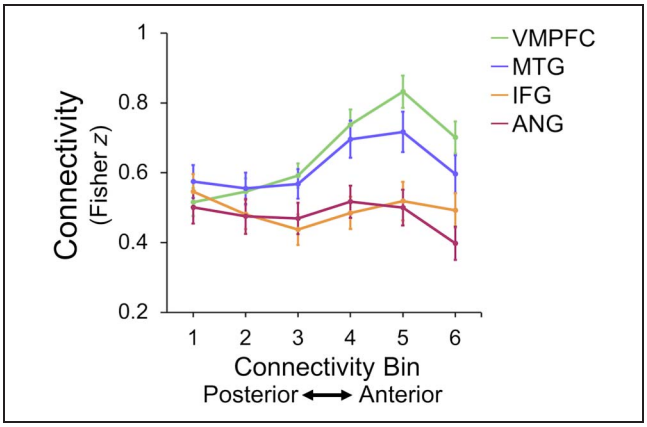

Figure 6. Continuous hippocampal connectivity. Hippocampal connectivity with each cortical region along a posterior to anterior gradient. Connectivity with VMPFC and MTG increased linearly from the posterior hippocampus to the anterior hippocampus. Each cortical region also revealed nonlinear trends.

regression analyses within each phase (rest, passive viewing, categorization; Figure 5). The connectivity–behavior relationship did not reach significance during the rest phase (all $|\beta| < .41$, $|t(21)| < 1.6$, $p > .14$), both anterior and posterior hippocampal–VMPFC connections were reliably related to performance during the passive viewing phase (anterior hippocampus: $\beta = -.59$, $t(21) = -2.78$, $p = .011$; posterior hippocampus: $\beta = -.44$, $t(21) = -2.12$, $p = .046$), and only anterior hippocampus–VMPFC connectivity reliably tracked performance during the categorization phase (anterior hippocampus: $\beta = -.43$, $t(21) = -2.31$, $p = .031$; posterior hippocampus: $\beta = -.31$, $t(21) = -1.23$, $p = .232$; Figure 5). However, although the relationship between VMPFC–hippocampus connectivity and performance was not significant in all phases, we did not find evidence that the strength of the relationship differed significantly across phases (all pairwise $|z| < 1.1$, all ps $> .3$). No other cortical region beyond VMPFC was implicated in the analyses of individual phases.

Continuous Hippocampal Connectivity

To test whether the observed differences in connectivity changed along the hippocampal long axis gradually or in a more step-wise fashion, we examined connectivity of each cortical region with individual cross-sectional hippocampal slices and then interpolated the connectivity values into six distinct bins. A 4 (Cortical ROI: ANG, IFG, VMPFC, MTG) × 6 (Hippocampal bin: labeled from posterior to anterior) repeated-measures ANOVA was conducted (Figure 6). Given that there was no three-way interaction between Hippocampal ROI, Cortical ROI, and Task phase in the ANOVA reported above, connectivity was averaged across the three tasks for this analysis. There was a main effect of Cortical ROI, $F(3, 75) = 22.83$, $p < .001$, $\eta_p^2 = .48$, and a main effect of Connectivity bin, $F(2.74, 68.55) = 15.37$, $p < .001$, $\eta_p^2 = .38$, GG, which were not of interest and not considered further. Of main interest, there was a significant interaction between Cortical ROI and Hippocampal bin, $F(5.26, 131.37) = 20.76$, $p < .001$, $\eta_p^2 = .45$, GG. To follow up on this interaction, we tested the effects of hippocampal bin using separate one-way, repeated-measures ANOVAs for each cortical ROI. In addition to the main effect of Hippocampal bin, linear and quadratic trends were of interest. We found main effects of hippocampal bin for all cortical ROIs: ANG, $F(3.07, 76.69) = 3.90$, $p = .011$, $\eta_p^2 = .14$, GG; IFG, $F(2.68, 66.91) = 4.19$, $p = .011$, $\eta_p^2 = .14$, GG; VMPFC, $F(2.82, 70.54) = 43.97$, $p < .001$, $\eta_p^2 = .64$, GG; and MTG, $F(2.33, 58.25) = 15.40$, $p < .001$, $\eta_p^2 = .38$, GG. There was a significant linear effect for both the VMPFC, $F(1, 25) = 76.54$, $p < .001$. $\eta_p^2 = .75$, and MTG, $F(1, 25) = 17.30$, $p < .001$, $\eta_p^2 = .41$, showing a gradient of increasing connectivity from posterior to anterior hippocampus. There was no linear effect of hippocampal bin in ANG, $F(1, 25) = 1.51$, $p = .230$, $\eta_p^2 = .06$, or IFG, $F(1, 25) = 0.19$, $p = .664$, $\eta_p^2 = .008$. Contrasts also revealed quadratic effects of hippocampal bin for IFG, $F(1, 25) = 16.22$, $p < .001$, $\eta_p^2 = .39$, and a marginal quadratic effect for ANG, $F(1, 25) = 3.70$, $p = .066$, but not for MTG or VMPFC (both $F < 3$, $p > .1$). The effects of connectivity bin partially replicated when we tested rest connectivity before low-pass filtering. Both MTG and VMPFC showed significant main effects of bin (both Fs > 5, both ps $< .005$), whereas ANG and IFG showed no effect of bin (both Fs < 2.5, both ps $> .1$).

Visual inspection of Figure 6 suggested that increases for MTG and VMPFC connectivity were not gradual but

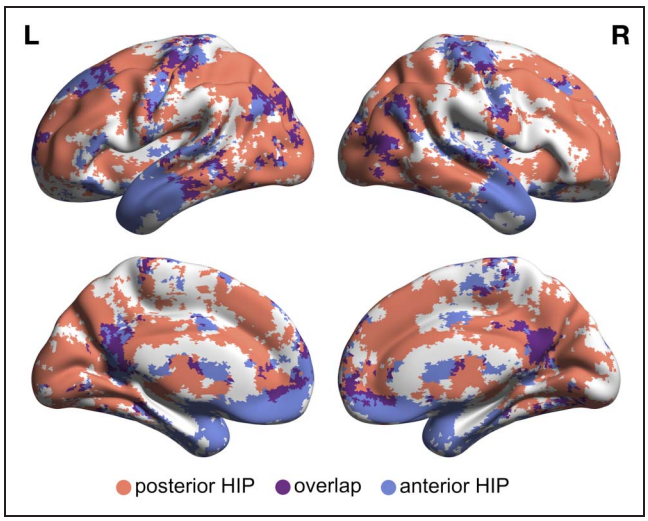

Figure 7. Whole-brain connectivity of the anterior and posterior hippocampus. Relative to the widely distributed hippocampal–cortical connectivity, there was little overlap in regions interacting with both anterior and posterior hippocampus.

Table 2. Anterior Hippocampal Connectivity

				Peak Coordinate		
	Hemisphere	*Voxels*	*z-Statistic*	*x*	*y*	*z*
Frontal lobe cluster		6643				
Ventromedial prefrontal cortex	L		6.97	−8	42	−14
Inferior frontal gyrus	L		6.27	−38	30	−18
Anterior cingulate gyrus	R	112	4.43	8	34	10
Superior frontal gyrus	L	57	4.17	−6	12	64
Precentral gyrus	R	34	4.54	6	−30	58
Postcentral/precentral gyrus	R	3506	5.83	56	−6	34
Postcentral gyrus	L	310	5.72	−36	−30	64
	R	279	5.4	30	−30	70
Central opercular cortex	R	230	4.85	48	−10	12
	R	190	4.83	56	−2	6
	L	69	4.86	−52	−10	12
Parietal operculum cortex	L	49	4.08	−48	−32	14
Posterior cingulate gyrus	R	1916	6.12	2	−48	30
Supramarginal gyrus	L	71	4.3	−62	−48	12
Temporal lobe cluster		6639				
Amygdala	L		6.61	−26	−4	−22
Anterior middle temporal gyrus	L		6.41	−58	2	−16
Parahippocampal cortex	L		6.35	−18	−16	−24
Temporal lobe cluster		5793				
Amygdala	R		8.09	36	59	28
Parahippocampal cortex	R		6.57	38	−12	−24
Temporal pole	R		6.48	48	16	−24
Superior lateral occipital cortex	L	592	5.71	−42	−72	32
	R	360	5	48	−66	32
	R	595	4.92	26	−86	14
	L	389	4.58	−30	−88	16
	L	75	4.93	−44	−76	34
Inferior lateral occipital cortex	L	127	4.59	−44	−82	0
Occipital fusiform gyrus	R	270	4.68	24	−62	−12
Fusiform cortex	L	66	4.34	−30	−62	−16
Lingual gyrus	L	76	4.29	−8	−78	−2
	L	45	4.44	−14	−76	−10
	L	34	4.38	−14	−90	−2

L = left; R = right.

Table 3. Posterior Hippocampal Connectivity

				Peak Coordinate		
	Hemisphere	*Voxels*	*z-Statistic*	*x*	*y*	*z*
Frontal lobe cluster		25244				
Anterior cingulate gyrus	R		6.89	4	34	24
Paracingulate gyrus	L		6.35	−4	32	26
Middle frontal gyrus	R		6.31	38	54	4
Paracingulate gyrus	R		6.22	6	46	−2
Lateral orbitofrontal cortex	L	51	3.95	−20	30	−18
Temporal lobe cluster		3374				
Inferior lateral occipital cortex	R		6.12	54	−70	−12
Posterior middle temporal gyrus	R		5.66	58	−34	−12
Temporal lobe cluster		2954				
Parahippocampal cortex	L		5.48	−34	−28	−18
Posterior middle temporal gyrus	L		5.42	−58	−30	−6
Fusiform cortex	L		5.41	−38	−64	−16
Temporal pole	L	98	5.3	−52	18	−10
	L	32	3.91	−52	16	−28
	R	40	3.97	52	−18	10
Parietal lobe cluster		19329				
Thalamus	L		6.62	−12	−36	0
Precuneus	L		6.24	−8	−78	50
Superior lateral occipital cortex	L		6.21	−28	−78	44
Precuneus	R		6.18	8	−62	18
Postcentral gyrus	L		4.18	−30	−30	58
Occippital lobe cluster		15167				
Occipital pole	L		6.4	−28	−92	12
Lingual gyrus	R		6.3	20	−60	−14
Superior lateral occipital cortex	L		6.28	−28	−80	44

L = left; R = right.

rather increased step-wise from the posterior half of the hippocampus (Bins 1–3) to the anterior half (Bins 4–6). In addition, there was a drop in connectivity for most regions with the most anterior bin. This observation was confirmed in MTG with post hoc pairwise comparisons between hippocampal bins, where Bins 1–3 showed equivalent connectivity (all pairwise ps $> .3$), whereas Bins 4–6 showed greater connectivity with MTG than Bins 1–3 (all ps $< .02$). The changes between Bins 3 and 4 were the largest increases in connectivity between neighboring bins (Fisher z increase = .128, SE = .024, $p < .001$). In VMPFC, connectivity values differed significantly across all pairs of bins (all ps $< .015$), except for most posterior Bins 1 and 2 ($p = .135$) and Bins 4 and 6 ($p = .383$). The greatest change of connectivity between neighboring bins was again between Bins 3 and 4 (Fisher z increase = 0.146, SE = 0.022, $p < .001$). Bin-to-bin connectivity changes in the IFG were reliably quadratic, with significant decreases from Bins 1–3 (all ps $< .05$) and marginal increases from Bins 3–5 (all ps $< .07$). Connectivity changes in ANG were less pronounced from bin to bin, though there was a significant change

Table 4. Anterior and Posterior Hippocampus Connectivity Overlap

Region	*Hemisphere*	*Cluster Size*
Paracingulate gyrus/superior frontal gyrus	M	1153
Frontal orbital cortex	L	10
	R	23
Frontal orbital cortex/inferior frontal gyrus	L	13
Rostral anterior cingulate cortex	M	24
	M	89
Dorsal anterior cingulate cortex	M	44
Caudate	R	11
	L	89
Thalamus	M	32
Precuneus/posterior cingulate gyrus	M	1381
Superior frontal/ middle frontal gyrus	R	75
	L	298
Superior frontal gyrus	L/M	18
Precentral gyrus	M	52
Precentral/postcentral gyrus	R	111
	L	905
	R	444
Insular cortex	R	14
	R	20
Parietal operculum cortex	R	10
Planum temporale	L	20
Superior temporal/middle temporal gyrus	R	265
Middle temporal gyrus	R	19
Middle temporal gyrus/inferior temporal gyrus	L	686
Temporal fusiform cortex/ parahippocampal cortex	R	17
Parahippocampal cortex	L	85
Temporal occipital fusiform cortex	R	52
	L	28
Temporal occipital fusiform cortex/occipital fusiform gyrus	L	28
	L	16
Occipital fusiform gyrus	R	358
Lingual gyrus	L	14
	L	35
	L	16
Lateral occipital cortex	R	696
	L	88
	L	681

Regions of overlap were defined in a conjunction analysis of anterior and posterior whole-brain connectivity maps.

from Bin 3 to Bin 4 and from Bin 5 to Bin 6 (both $ps < .03$).

Whole-brain Connectivity of Anterior and Posterior Hippocampus

We next examined whole-brain connectivity maps for the anterior and posterior hippocampus and the degree of their overlap. As anterior versus posterior hippocampal connectivity differences did not significantly vary across task phases in the prior analyses, our report is limited to connectivity averaged across the three phases. The anterior and posterior hippocampus showed widespread cortical connectivity (Figure 7). Anterior hippocampus was correlated with portions of the VMPFC, anterior lateral temporal cortices, and lateral orbitofrontal cortices (Table 2). Posterior hippocampus formed a larger network of regions that included lateral pFC, dorsomedial pFC, lateral parietal cortices, and posterior temporal and occipital visual cortices (Table 3). Though anterior and posterior hippocampal connectivity maps jointly spanned much of the cortex, there was relatively little overlap (Figure 7). Regions that interacted with both anterior and posterior hippocampus included medial pFC, anterior and posterior cingulate cortex, precuneus, portions of lateral temporal cortex, and portions of lateral occipital cortex (Table 4; Figure 7).

DISCUSSION

How does the hippocampus support memory for individual events and generalization across experiences? We tested whether distinct portions of the hippocampus (posterior vs. anterior) differentially interacted with portions of cortex that have been linked to memory specificity (ANG, IFG) versus those implicated in memory generalization (VMPFC, MTG). Consistent with their putative roles in memory specificity, we found that ANG and IFG were preferentially connected to the posterior

hippocampus. Consistent with their putative role in generalization, we found that the VMPFC and MTG were preferentially connected to the anterior hippocampus, although the effect in MTG was only apparent when connectivity was measured continuously along the long axis of the hippocampus. Individual differences in hippocampal–VMPFC connectivity tracked individual differences in concept generalization performance, but this relationship was not unique to the anterior portion of the hippocampus. Whole-brain connectivity analyses revealed widespread connectivity networks for anterior and posterior hippocampus, with relatively little overlap between them. Lastly, anterior and posterior hippocampal connectivity differences persisted across the three scanning phases and were apparent even at rest. This finding suggests that the anterior and posterior hippocampus may form distinct intrinsic functional networks that are relatively independent of task engagement.

A key finding of the current study is that anterior and posterior hippocampus have distinct connectivity profiles that persist across different levels of task engagement. The notion of long-axis specialization within hippocampus is not new. Several models have posited functional differences between anterior and posterior portions of the hippocampus in terms of vestibular versus visual processing (Hüfner, Strupp, Smith, Brandt, & Jahn, 2011), encoding versus retrieval (Kim, 2015; Lepage, Habib, & Tulving, 1998), and emotional versus cognitive processing (Fanselow & Dong, 2010). Anatomically, cellular and genetic differences exist between the two hippocampal divisions (Thompson et al., 2008), as do structural connectivity differences in humans (Adnan et al., 2016) and rodents (Fanselow & Dong, 2010; Moser & Moser, 1998). Human fMRI studies have also noted differences in the functional connectivity between the anterior and posterior hippocampus (Adnan et al., 2016; Blessing et al., 2016; Blum, Habeck, Steffener, Razlighi, & Stern, 2014; Poppenk & Moscovitch, 2011; Kahn, Andrews-Hanna, Vincent, Snyder, & Buckner, 2008; see also Poppenk et al., 2013, for a review). Here, we highlight a novel aspect of the anterior versus posterior dissociations within the hippocampus, demonstrating greater anterior hippocampal connectivity with putative memory generalization regions and greater posterior hippocampal connectivity with putative memory specificity regions. These findings align well with a recent model of representational gradient along the long axis of the hippocampus proposed by Poppenk et al. (2013), postulating fine-grained representations in the posterior hippocampus and coarse-grained representations in the anterior hippocampus. As such, the posterior hippocampus may be especially suited for retaining differentiating details of individual experiences on fine spatial and temporal scales whereas anterior hippocampus may be especially suited for aggregating information across events to support generalization (Bowman & Zeithamova, 2018; Brunec et al., 2018; Schlichting et al., 2015). The novel evidence that the anterior and posterior hippocampus form distinct functional connections with cortical regions differentially supporting memory specificity and generalization provides one mechanism for how these complementary memory functions may both be served by the hippocampus.

A large body of past research has implicated the ANG and IFG in maintaining specific memory representations, with the IFG resolving interference between related items (Bowman & Dennis, 2015, 2016; Kuhl et al., 2007; Achim & Lepage, 2005; Badre, Poldrack, Paré-Blagoev, Insler, & Wagner, 2005; Jonides et al., 1998) and ANG supporting detailed retrieval of past events (Lee, Samide, Richter, & Kuhl, 2018; Xiao et al., 2017; Richter, Cooper, Bays, & Simons, 2016; Kuhl & Chun, 2014; Johnson, Suzuki, & Rugg, 2013; Vilberg & Rugg, 2007). As such, we predicted that if the critical difference in anterior versus posterior hippocampal function were one of representational granularity, the posterior hippocampus would show stronger functional connectivity with these regions than would the anterior hippocampus. The results were consistent with this prediction, indicating that the posterior hippocampus may be more strongly geared toward fine-grained representations both because of the computational properties of its cells (Kjelstrup et al., 2008) and its functional interactions with cortical regions that support differentiation between overlapping memories.

Prior studies have shown that the VMPFC and MTG support multiple forms of memory generalization, including concept generalization (Bowman & Zeithamova, 2018; Davis, Goldwater, & Giron, 2017), false memories (Turney & Dennis, 2017; Garoff-Eaton, Slotnick, & Schacter, 2006), and schema-based memories (Brod, Lindenberger, Werkle-Bergner, & Shing, 2015; van Kesteren et al., 2013). Based on the notion that representations in the anterior hippocampus are broad and well suited to integrating across experiences (Brunec et al., 2018; Collin et al., 2015), we expected—and found—greater functional connectivity of VMPFC and MTG with the anterior than posterior hippocampus. The VMPFC findings are consistent with work showing that hippocampal–VMPFC interactions support linking of related information in memory (Gerraty et al., 2014; Zeithamova et al., 2012; van Kesteren et al., 2010) and provide novel evidence that the VMPFC interactions are particularly strong with the anterior portion of the hippocampus. The MTG showed numerically stronger connectivity with anterior compared with posterior hippocampus, although this relationship was only significant when connectivity was measured continuously. Although the role of lateral temporal cortices in semantic memory has long been known (Mummery et al., 1999, 2000), they have only recently been linked to a VMPFC–hippocampal network that supports learning based on prior knowledge (Liu et al., 2017). The present findings add to this work by demonstrating that both VMPFC and MTG are more strongly connected to the anterior hippocampus, both in the context of a concept generalization task and during rest.

Linking connectivity strength with concept generalization performance, individual differences in hippocampal–VMPFC connectivity tracked categorization success. These results corroborate prior reports linking VMPFC activation to the formation of conceptual knowledge (Kumaran et al., 2009; Zeithamova, Maddox, & Schnyer, 2008), including generalized concept representations (Bowman & Zeithamova, 2018). Prior work has also implicated VMPFC–hippocampal interactions in some forms of memory generalization, such as narrative schema formation (van Kesteren et al., 2010), associative inference (Zeithamova et al., 2012), and transfer of reward valence across related stimuli (Gerraty et al., 2014). The current work extends the work on VMPFC–hippocampal interactions to the new domain of concept generalization, indicating that they may serve to link information across experiences to serve many forms of memory generalization. Additionally, we also show the relative stability of the connectivity–behavior relationship that did not significantly differ across phases, although it was most prominent during task performance specifically.

An interesting observation is the negative direction of the relationship between generalization success and VMPFC–hippocampus connectivity strength observed here, as well as in two prior reports (Gerraty et al., 2014; van Kesteren et al., 2010), with stronger connectivity being associated with poorer generalization. These connectivity findings contrast with findings that involve task-based activations and show its positive relationship to generalization performance (Kumaran et al., 2009; Zeithamova et al., 2008). The mechanisms of this negative connectivity–behavior relationship remain unclear. VMPFC–hippocampal connectivity seems to be increasing when a schema linking previously separate events needs to be formed (van Kesteren et al., 2010; see also Zeithamova et al., 2012). Thus, one possibility is that low baseline or postencoding connectivity reflects that information has been already successfully linked. Gerraty et al. (2014) measured connectivity based on a rest scan conducted on a separate day from when participants underwent an associative learning and transfer task. Thus, lower resting/baseline VMPFC–hippocampal connectivity could also reflect a trait-like property of this network that makes it open to on-demand engagement in new schema learning. Pending further investigation and better insights into the mechanisms reflected in VMPFC–hippocampal functional connectivity, the reasons behind the negative correlation–behavior relationship remain speculative.

Although VMPFC–anterior hippocampus connectivity was the strongest predictor of concept generalization success, the data did not indicate the connectivity–behavior relationship to be unique to the anterior hippocampus. Posterior hippocampus–VMPFC connectivity, although not reaching significance overall, showed a similar trend. Prior work has demonstrated that related events may be encoded as integrated or separated representations (Chanales, Oza, Favila, & Kuhl, 2017; Zeithamova & Preston, 2010, 2017; Schlichting et al., 2015). Thus, within the framework of representational granularity along the long hippocampal axis, one may speculate that these connections reflect different process. For example, information represented in both portions of the hippocampus may be relevant to generalization decisions but differentially reflect reliance on specific versus generalized representations. Alternatively, the posterior hippocampus–VMPFC interactions may reflect postencoding linking of previously separated representations that are then encoded in the anterior hippocampus. However, whether the posterior and anterior hippocampal connectivity with VMPFC reflects the same or distinct processes cannot be answered based on the current data. As noted above, the sample size was not optimized for an individual difference analysis, and thus, the findings linking connectivity to behavior should be replicated in a larger study.

Finding anterior versus posterior differences, we further asked whether hippocampal–cortical functional connectivity was graded along the long axis or if instead there was a stepwise increase at an anterior/posterior boundary. The results did not show a clear pattern of graded changes along the hippocampal long axis and instead pointed to more complex patterns. In particular, both the VMPFC and MTG showed a stepwise increase from the posterior half to the anterior half of the hippocampus. The IFG showed a quadratic effect, which may represent differences in hippocampal anatomy, such as the relative distribution of hippocampal subfields (Malykhin, Lebel, Coupland, Wilman, & Carter, 2010) or the relative density of structural connections to other brain regions (Shepherd, Özarslan, King, Mareci, & Blackband, 2006; Dolorfo & Amaral, 1998). For the most anterior bin, the weaker connectivity detected here across multiple ROIs likely reflects differences in shape, reduced number of voxels, and/or differences in signal to noise in this portion of the hippocampus (Brunec et al., 2018). Nonlinearities may have also arisen from functional heterogeneity within the cortical regions themselves. For example, the IFG has anatomical subregions that may perform distinct computations that are differentially relevant for memory specificity and generalization (Badre & Wagner, 2007; Gold et al., 2006; Badre et al., 2005), possibly leading to differences in connectivity with the hippocampus. Thus, it remains an open question whether these nonlinear effects are driven by differences within the hippocampus, the cortical ROIs, or by some other factor.

Across most analyses, we found little evidence that hippocampal connectivity patterns were modulated by task engagement. Rather, anterior and posterior hippocampal connectivity differences were present across all phases, including unfiltered rest data. Thus, it seems that differences in anterior and posterior connectivity are not driven by task demands but are instead relatively stable characteristics of hippocampal networks. These results extend prior findings on resting-state connectivity differences between anterior and posterior hippocampus (Adnan et al., 2016; Blessing et al., 2016; Blum et al., 2014; Poppenk &

Moscovitch, 2011; Kahn et al., 2008) to show that differences in anterior and posterior hippocampal connectivity persist even under passive and active task demands. These results are consistent with recent notions of the traitlike properties of functional connectivity patterns detectable across time and tasks (Frank et al., 2019; Horien et al., 2019; Gratton et al., 2018; Touroutoglou et al., 2015). Our findings of stable connectivity patterns complement prior studies that have examined connectivity in the context of categorization but focused on task-related connectivity changes (Turner, Crossley, & Ashby, 2017; Mack, Love, & Preston, 2016; Soto, Bassett, & Ashby, 2016; Seger & Cincotta, 2006). Together, these results highlight that both task-related connectivity changes and stable connectivity patterns carry information relevant to our understanding on how the brain supports cognition.

Our findings of stable functional connectivity differences between anterior and posterior hippocampus may more broadly reflect their structural connectivity profiles. Rodent and primate literature have shown distinct structural connectivity between anterior (ventral) and posterior (dorsal) hippocampus both within the medial-temporal lobe (Fanselow & Dong, 2010; Suzuki & Amaral, 1994) and across the cortex (Catenoix, Magnin, Mauguière, & Ryvlin, 2011; Kier, Staib, Davis, & Bronen, 2004). Moreover, our pattern of findings is relatively consistent with structural connections of anterior and posterior hippocampus. In humans, white matter tracts connect anterior hippocampus with VMPFC and anterior lateral temporal cortices (Catenoix et al., 2011; Kier et al., 2004). The body and tail of the hippocampus are connected to parietal regions through more complex pathways (Duvernoy, Cattin, Risold, Vannson, & Gaudron, 2013), but direct connections exist between ANG and posterior portions of the medial-temporal lobe surrounding the hippocampus (Uddin et al., 2010; Rushworth, Behrens, & Johansen-Berg, 2006). IFG forms connections that span the entire hippocampus (Oishi et al., 2008; Kier et al., 2004). Though future investigation is required, our findings of functional connectivity differences between anterior and posterior hippocampus may arise from differences in structural connections.

The IFG was one exception to the otherwise stable connectivity, showing increased connectivity from rest to task (both passive viewing and categorization). IFG is part of a larger frontoparietal network that orients attention to behaviorally relevant stimuli (Raichle, Fox, Corbetta, Snyder, & Vincent, 2006; Corbetta & Shulman, 2002) and increases in activation when participants engage in an externally oriented task compared with rest or an internally oriented task (Scheibner, Bogler, Gleich, Haynes, & Bermpohl, 2017; Spreng, Stevens, Chamberlain, Gilmore, & Schacter, 2010; Cabeza & Nyberg, 2000). The nature of the task at hand may dictate the degree to which hippocampus interacts with IFG, as has been reported for hippocampal interactions with the frontoparietal control network (Westphal, Wang, & Rissman, 2017). The IFG is also recruited for learning statistical regularities in the temporal sequence of stimuli (Schapiro, Turk-Browne, Norman, & Botnivick, 2016; Karuza et al., 2013; Schapiro, Rogers, Cordova, Turk-Browne, & Botvinick, 2013), with hippocampal–IFG connectivity modulated at boundaries in the temporal structure (Schapiro et al., 2016). Thus, hippocampal–IFG connectivity may more strongly reflect dynamic task demands than stable traits of individuals. However, it is not possible to rule out that what we interpret as task-related increases in background connectivity may be to some degree driven by coactivation related to task features occurring below the filter cutoff frequency.

The current findings are complementary to other frameworks that propose hippocampal interactions with distinct networks to serve multiple memory functions. For example, Ranganath and Ritchey (2012) propose that the hippocampus interacts with two medial-temporal lobe networks: a posterior-medial network that includes the parahippocampal cortex and represents the spatial and temporal context of memory and an anterior-temporal network that includes perirhinal cortex and represents individual items and their features. The hippocampus integrates item and contextual information into a coherent representation (Diana, Yonelinas, & Ranganath, 2007). Consistent with this proposed function, Cooper and Ritchey (2019) found increased connectivity between the hippocampus and both posterior-medial and anterior-temporal networks during retrieval of memories with multidimensional features (i.e., spatial, visual and emotional), with connectivity increases scaling with the quality of memory retrieval. Interestingly, differences emerged along the hippocampal axis such that posterior hippocampal connectivity with both medial-temporal lobe networks demonstrated greater scaling with retrieval quality, which would be consistent with its hypothesized role in memory specificity. How these different conceptualizations of distinct hippocampal functions complement or interact with each other is an interesting area for future research.

The current study provides novel evidence for differential functional interactions along the hippocampal long axis, showing distinctions in connectivity patterns of anterior versus posterior hippocampus with cortical regions that align with their putative role in memory specificity and generalization and that persist across levels of task engagement. The distinct cortical interactions with anterior and posterior hippocampus may provide one mechanism for how a single region—the hippocampus—may form both specific and generalized representations supporting multiple memory functions. More broadly, the findings add to our understanding of functional organization along the hippocampal long axis and highlight the utility of functional connectivity measures in the study of cognition.

Reprint requests should be sent to Dagmar Zeithamova, University of Oregon, 1227 University St., Eugene, OR 97403, or via e-mail: dasa@uoregon.edu.

REFERENCES

Achim, A. M., & Lepage, M. (2005). Dorsolateral prefrontal cortex involvement in memory post-retrieval monitoring revealed in both item and associative recognition tests. *Neuroimage*, *24*, 1113–1121.

Adnan, A., Barnett, A., Moayedi, M., McCormick, C., Cohn, M., & McAndrews, M. P. (2016). Distinct hippocampal functional networks revealed by tractography-based parcellation. *Brain Structure and Function*, *221*, 2999–3012.

Al-Aidroos, N., Said, C. P., & Turk-Browne, N. B. (2012). Top–down attention switches coupling between low-level and high-level areas of human visual cortex. *Proceedings of the National Academy of Sciences, U.S.A.*, *109*, 14675–14680.

Andrews-Hanna, J. R., Reidler, J. S., Sepulcre, J., Poulin, R., & Buckner, R. L. (2010). Functional-anatomic fractionation of the brain's default network. *Neuron*, *65*, 550–562.

Badre, D., Poldrack, R. A., Paré-Blagoev, E. J., Insler, R. Z., & Wagner, A. D. (2005). Dissociable controlled retrieval and generalized selection mechanisms in ventrolateral prefrontal cortex. *Neuron*, *47*, 907–918.

Badre, D., & Wagner, A. D. (2005). Frontal lobe mechanisms that resolve proactive interference. *Cerebral Cortex*, *15*, 2003–2012.

Badre, D., & Wagner, A. D. (2007). Left ventrolateral prefrontal cortex and the cognitive control of memory. *Neuropsychologia*, *45*, 2883–2901.

Berens, S. C., & Bird, C. M. (2017). The role of the hippocampus in generalizing configural relationships. *Hippocampus*, *27*, 223–228.

Blessing, E. M., Beissner, F., Schumann, A., Brünner, F., & Bär, K. J. (2016). A data-driven approach to mapping cortical and subcortical intrinsic functional connectivity along the longitudinal hippocampal axis. *Human Brain Mapping*, *37*, 462–476.

Blum, S., Habeck, C., Steffener, J., Razlighi, Q., & Stern, Y. (2014). Functional connectivity of the posterior hippocampus is more dominant as we age. *Cognitive Neuroscience*, *5*, 150–159.

Bowman, C. R., & Dennis, N. A. (2015). The neural correlates of correctly rejecting lures during memory retrieval: The role of item relatedness. *Experimental Brain Research*, *233*, 1963–1975.

Bowman, C. R., & Dennis, N. A. (2016). The neural basis of recollection rejection: Increases in hippocampal–prefrontal connectivity in the absence of a shared recall-to-reject and target recollection network. *Journal of Cognitive Neuroscience*, *28*, 1194–1209.

Bowman, C. R., & Zeithamova, D. (2018). Abstract memory representations in the ventromedial prefrontal cortex and hippocampus support concept generalization. *Journal of Neuroscience*, *38*, 2605–2614.

Brod, G., Lindenberger, U., Werkle-Bergner, M., & Shing, Y. L. (2015). Differences in the neural signature of remembering schema-congruent and schema-incongruent events. *Neuroimage*, *117*, 358–366.

Brunec, I. K., Bellana, B., Ozubko, J. D., Man, V., Robin, J., Liu, Z.-X., et al. (2018). Multiple scales of representation along the hippocampal anteroposterior axis in humans. *Current Biology*, *28*, 2129–2135.

Bunsey, M., & Eichenbaum, H. (1996). Conservation of hippocampal memory function in rats and humans. *Nature*, *379*, 255–257.

Cabeza, R., & Nyberg, L. (2000). Imaging cognition II: An empirical review of 275 PET and fMRI studies. *Journal of Cognitive Neuroscience*, *12*, 1–47.

Catenoix, H., Magnin, M., Mauguière, F., & Ryvlin, P. (2011). Evoked potential study of hippocampal efferent projections in the human brain. *Clinical Neurophysiology*, *122*, 2488–2497.

Chanales, A. J. H., Oza, A., Favila, S. E., & Kuhl, B. A. (2017). Overlap among spatial memories triggers repulsion of hippocampal representations. *Current Biology*, *27*, 2307–2317.

Collin, S. H. P., Milivojevic, B., & Doeller, C. F. (2015). Memory hierarchies map onto the hippocampal long axis in humans. *Nature Neuroscience*, *18*, 1562–1564.

Cooper, R. A., & Ritchey, M. (2019). Cortico-hippocampal network connections support the multidimensional quality of episodic memory. *ELife*, *8*, e45591.

Corbetta, M., & Shulman, G. L. (2002). Control of goal-directed and stimulus-driven attention in the brain. *Nature Reviews: Neuroscience*, *3*, 201–215.

Davis, T., Goldwater, M., & Giron, J. (2017). From concrete examples to abstract relations: The rostrolateral prefrontal cortex integrates novel examples into relational categories. *Cerebral Cortex*, *27*, 2652–2670.

Davis, T., & Poldrack, R. A. (2014). Quantifying the internal structure of categories using a neural typicality measure. *Cerebral Cortex*, *24*, 1720–1737.

Dennis, N. A., Kim, H., & Cabeza, R. (2008). Age-related differences in brain activity during true and false memory retrieval. *Journal of Cognitive Neuroscience*, *20*, 1390–1402.

Destrieux, C., Fischl, B., Dale, A., & Halgren, E. (2010). Automatic parcellation of human cortical gyri and sulci using standard anatomical nomenclature. *Neuroimage*, *53*, 1–15.

Diana, R. A., Yonelinas, A. P., & Ranganath, C. (2007). Imaging recollection and familiarity in the medial temporal lobe: A three-component model. *Trends in Cognitive Sciences*, *11*, 379–386.

Dolorfo, C. L., & Amaral, D. G. (1998). Entorhinal cortex of the rat: Topographic organization of the cells of origin of the perforant path projection to the dentate gyrus. *Journal of Comparative Neurology*, *398*, 25–48.

Duncan, K., Tompary, A., & Davachi, L. (2014). Associative encoding and retrieval are predicted by functional connectivity in distinct hippocampal area CA1 pathways. *Journal of Neuroscience*, *34*, 11188–11198.

Duvernoy, H. M., Cattin, F., Risold, P. Y., Vannson, J. L., & Gaudron, M. (2013). *The human hippocampus: Functional anatomy, vascularization and serial sections with MRI* (4th ed.). Berlin/Heidelberg: Springer.

Fanselow, M. S., & Dong, H.-W. (2010). Are the dorsal and ventral hippocampus functionally distinct structures? *Neuron*, *65*, 7–19.

Frank, L. E., Preston, A. R., & Zeithamova, D. (2019). Functional connectivity between memory and reward centers across task and rest track memory sensitivity to reward. *Cognitive Affective and Behavioral Neuroscience*, *19*, 503–522.

Garoff-Eaton, R. J., Slotnick, S. D., & Schacter, D. L. (2006). Not all false memories are created equal: The neural basis of false recognition. *Cerebral Cortex*, *16*, 1645–1652.

Gerraty, R. T., Davidow, J. Y., Wimmer, G. E., Kahn, I., & Shohamy, D. (2014). Transfer of learning relates to intrinsic connectivity between hippocampus, ventromedial prefrontal cortex, and large-scale networks. *Journal of Neuroscience*, *34*, 11297–11303.

Gold, B. T., Balota, D. A., Jones, S. J., Powell, D. K., Smith, C. D., & Andersen, A. H. (2006). Dissociation of automatic and strategic lexical-semantics: Functional magnetic resonance imaging evidence for differing roles of multiple frontotemporal regions. *Journal of Neuroscience*, *26*, 6523–6532.

Gratton, C., Laumann, T. O., Nielsen, A. N., Greene, D. J., Gordon, E. M., Gilmore, A. W., et al. (2018). Functional brain networks are dominated by stable group and individual

factors, not cognitive or daily variation. *Neuron*, *98*, 439–452.
Horien, C., Shen, X., Scheinost, D., & Constable, R. T. (2019). The individual functional connectome is unique and stable over months to years. *Neuroimage*, *189*, 676–687.
Hüfner, K., Strupp, M., Smith, P., Brandt, T., & Jahn, K. (2011). Spatial separation of visual and vestibular processing in the human hippocampal formation. *Annals of the New York Academy of Sciences*, *1233*, 177–186.
Johnson, J. D., Suzuki, M., & Rugg, M. D. (2013). Recollection, familiarity, and content-sensitivity in lateral parietal cortex: A high-resolution fMRI study. *Frontiers in Human Neuroscience*, *7*, 219.
Jonides, J., Smith, E. E., Marshuetz, C., Koeppe, R. A., & Reuter-Lorenz, P. A. (1998). Inhibition in verbal working memory revealed by brain activation. *Proceedings of the National Academy of Sciences, U.S.A.*, *95*, 8410–8413.
Kahn, I., Andrews-Hanna, J. R., Vincent, J. L., Snyder, A. Z., & Buckner, R. L. (2008). Distinct cortical anatomy linked to subregions of the medial temporal lobe revealed by intrinsic functional connectivity. *Journal of Neurophysiology*, *100*, 129–139.
Karuza, E. A., Newport, E. L., Aslin, R. N., Starling, S. J., Tivarus, M. E., & Bavelier, D. (2013). The neural correlates of statistical learning in a word segmentation task: An fMRI study. *Brain and Language*, *127*, 46–54.
Kier, E. L., Staib, L. H., Davis, L. M., & Bronen, R. A. (2004). MR imaging of the temporal stem: Anatomic dissection tractography of the uncinate fasciculus, inferior occipitofrontal fasciculus, and Meyer's loop of the optic radiation. *American Journal of Neuroradiology*, *25*, 677–691.
Kim, H. (2015). Encoding and retrieval along the long axis of the hippocampus and their relationships with dorsal attention and default mode networks: The HERNET model. *Hippocampus*, *25*, 500–510.
Kjelstrup, K. B., Solstad, T., Brun, V. H., Hafting, T., Leutgeb, S., Witter, M. P., et al. (2008). Finite scale of spatial representation in the hippocampus. *Science*, *321*, 140–143.
Kuhl, B. A., & Chun, M. M. (2014). Successful remembering elicits event-specific activity patterns in lateral parietal cortex. *Journal of Neuroscience*, *34*, 8051–8060.
Kuhl, B. A., Dudukovic, N. M., Kahn, I., & Wagner, A. D. (2007). Decreased demands on cognitive control reveal the neural processing benefits of forgetting. *Nature Neuroscience*, *10*, 908–914.
Kumaran, D., Summerfield, J. J., Hassabis, D., & Maguire, E. A. (2009). Tracking the emergence of conceptual knowledge during human decision making. *Neuron*, *63*, 889–901.
Lee, H., Samide, R., Richter, F. R., & Kuhl, B. A. (2018). Decomposing parietal memory reactivation to predict consequences of remembering. *Cerebral Cortex*, *29*, 3305–3318.
Lepage, M., Habib, R., & Tulving, E. (1998). Hippocampal PET activations of memory encoding and retrieval: The HIPER model. *Hippocampus*, *8*, 313–322.
Liu, Z. X., Grady, C., & Moscovitch, M. (2017). Effects of prior-knowledge on brain activation and connectivity during associative memory encoding. *Cerebral Cortex*, *27*, 1991–2009.
Liu, Z. X., Grady, C., & Moscovitch, M. (2018). The effect of prior knowledge on post-encoding brain connectivity and its relation to subsequent memory. *Neuroimage*, *167*, 211–223.
Mack, M. L., Love, B. C., & Preston, A. R. (2016). Dynamic updating of hippocampal object representations reflects new conceptual knowledge. *Proceedings of the National Academy of Sciences, U.S.A.*, *113*, 13203–13208.
Malykhin, N. V., Lebel, R. M., Coupland, N. J., Wilman, A. H., & Carter, R. (2010). In vivo quantification of hippocampal subfields using 4.7 T fast spin echo imaging. *Neuroimage*, *49*, 1224–1230.
Manelis, A., Paynter, C. A., Wheeler, M. E., & Reder, L. M. (2013). Repetition related changes in activation and functional connectivity in hippocampus predict subsequent memory. *Hippocampus*, *23*, 53–65.
Moser, M. B., & Moser, E. I. (1998). Functional differentiation in the hippocampus. *Hippocampus*, *8*, 608–619.
Mummery, C. J., Patterson, K., Price, C. J., Ashburner, J., Frackowiak, R. S., & Hodges, J. R. (2000). A voxel-based morphometry study of semantic dementia: Relationship between temporal lobe atrophy and semantic memory. *Annals of Neurology*, *47*, 36–45.
Mummery, C. J., Patterson, K., Wise, R. J., Vandenbergh, R., Price, C. J., & Hodges, J. R. (1999). Disrupted temporal lobe connections in semantic dementia. *Brain*, *122*, 61–73.
Murphy, K., Birn, R. M., & Bandettini, P. A. (2013). Resting-state fMRI confounds and cleanup. *Neuroimage*, *80*, 349–359.
Norman-Haignere, S. V., McCarthy, G., Chun, M. M., & Turk-Browne, N. B. (2012). Category-selective background connectivity in ventral visual cortex. *Cerebral Cortex*, *22*, 391–402.
Oishi, K., Zilles, K., Amunts, K., Faria, A., Jiang, H., Li, X., et al. (2008). Human brain white matter atlas: Identification and assignment of common anatomical structures in superficial white matter. *Neuroimage*, *43*, 447–457.
Poppenk, J., Evensmoen, H. R., Moscovitch, M., & Nadel, L. (2013). Long-axis specialization of the human hippocampus. *Trends in Cognitive Sciences*, *17*, 230–240.
Poppenk, J., & Moscovitch, M. (2011). A hippocampal marker of recollection memory ability among healthy young adults: Contributions of posterior and anterior segments. *Neuron*, *72*, 931–937.
Power, J. D., Barnes, K. A., Snyder, A. Z., Schlaggar, B. L., & Petersen, S. E. (2012). Spurious but systematic correlations in functional connectivity MRI networks arise from subject motion. *Neuroimage*, *59*, 2142–2154.
Raichle, M. E., Fox, M. D., Corbetta, M., Snyder, A. Z., & Vincent, J. L. (2006). Spontaneous neuronal activity distinguishes human dorsal and ventral attention systems. *Proceedings of the National Academy of Sciences, U.S.A.*, *103*, 10046–10051.
Ranganath, C., & Ritchey, M. (2012). Two cortical systems for memory-guided behaviour. *Nature Reviews: Neuroscience*, *13*, 713–726.
Richter, F. R., Cooper, R. A., Bays, P. M., & Simons, J. S. (2016). Distinct neural mechanisms underlie the success, precision, and vividness of episodic memory. *eLife*, *5*, e18260.
Robinson, J. L., Salibi, N., & Deshpande, G. (2016). Functional connectivity of the left and right hippocampi: Evidence for functional lateralization along the long-axis using meta-analytic approaches and ultra-high field functional neuroimaging. *Neuroimage*, *135*, 64–78.
Rushworth, M. F. S., Behrens, T. E. J., & Johansen-Berg, H. (2006). Connection patterns distinguish 3 regions of human parietal cortex. *Cerebral Cortex*, *16*, 1418–1430.
Schapiro, A. C., Rogers, T. T., Cordova, N. I., Turk-Browne, N. B., & Botvinick, M. M. (2013). Neural representations of events arise from temporal community structure. *Nature Neuroscience*, *16*, 486–492.
Schapiro, A. C., Turk-Browne, N. B., Botvinick, M. M., & Norman, K. A. (2017). Complementary learning systems within the hippocampus: A neural network modelling approach to reconciling episodic memory with statistical learning. *Philosophical Transactions of the Royal Society, Series B: Biological Sciences*, *372*, 20160049.
Schapiro, A. C., Turk-Browne, N. B., Norman, K. A., & Botnivick, M. M. (2016). Statistical learning of temporal community structure in the hippocampus. *Hippocampus*, *26*, 3–8.

Scheibner, H. J., Bogler, C., Gleich, T., Haynes, J. D., & Bermpohl, F. (2017). Internal and external attention and the default mode network. *Neuroimage*, *148*, 381–389.
Schlichting, M. L., Mumford, J. A., & Preston, A. R. (2015). Learning-related representational changes reveal dissociable integration and separation signatures in the hippocampus and prefrontal cortex. *Nature Communications*, *6*, 8151.
Scoville, W. B., & Milner, B. (1957). Loss of recent memory after bilateral hippocampal lesions. *Journal of Neuropsychiatry and Clinical Neurosciences*, *20*, 11–21.
Seger, C. A., & Cincotta, C. M. (2006). Dynamics of frontal, striatal, and hippocampal systems during rule learning. *Cerebral Cortex*, *16*, 1546–1555.
Shepherd, T. M., Özarslan, E., King, M. A., Mareci, T. H., & Blackband, S. J. (2006). Structural insights from high-resolution diffusion tensor imaging and tractography of the isolated rat hippocampus. *Neuroimage*, *32*, 1499–1509.
Shohamy, D., & Wagner, A. D. (2008). Integrating memories in the human brain: Hippocampal-midbrain encoding of overlapping events. *Neuron*, *60*, 378–389.
Soto, F. A., Bassett, D. S., & Ashby, F. G. (2016). Dissociable changes in functional network topology underlie early category learning and development of automaticity. *Neuroimage*, *141*, 220–241.
Spreng, R. N., Stevens, W. D., Chamberlain, J. P., Gilmore, A. W., & Schacter, D. L. (2010). Default network activity, coupled with the frontoparietal control network, supports goal-directed cognition. *Neuroimage*, *53*, 303–317.
Steiger, J. H. (1980). Tests for comparing elements of a correlation matrix. *Psychological Bulletin*, *87*, 245–251.
Suzuki, W., & Amaral, D. (1994). Topographic organization of the reciprocal connections between the monkey entorhinal cortex and the perirhinal and parahippocampal cortices. *Journal of Neuroscience*, *14*, 1856–1877.
Tambini, A., Nee, D. E., & D'Esposito, M. (2017). Hippocampal-targeted theta-burst stimulation enhances associative memory formation. *Journal of Cognitive Neuroscience*, *30*, 1452–1472.
Tambini, A., Rimmele, U., Phelps, E. A., & Davachi, L. (2017). Emotional brain states carry over and enhance future memory formation. *Nature Neuroscience*, *20*, 271–278.
Thompson, C. L., Pathak, S. D., Jeromin, A., Ng, L. L., MacPherson, C. R., Mortrud, M. T., et al. (2008). Genomic anatomy of the hippocampus. *Neuron*, *60*, 1010–1021.
Touroutoglou, A., Andreano, J. M., Barrett, L. F., & Dickerson, B. C. (2015). Brain network connectivity–behavioral relationships exhibit trait-like properties: Evidence from hippocampal connectivity and memory. *Hippocampus*, *25*, 1591–1598.
Turner, B. O., Crossley, M. J., & Ashby, F. G. (2017). Hierarchical control of procedural and declarative category-learning systems. *Neuroimage*, *150*, 150–161.
Turney, I. C., & Dennis, N. A. (2017). Elucidating the neural correlates of related false memories using a systematic measure of perceptual relatedness. *Neuroimage*, *146*, 940–950.
Uddin, L. Q., Supekar, K., Amin, H., Rykhlevskaia, E., Nguyen, D. A., Greicius, M. D., et al. (2010). Dissociable connectivity within human angular gyrus and intraparietal sulcus: Evidence from functional and structural connectivity. *Cerebral Cortex*, *20*, 2636–2646.
Van Dijk, K. R. A., Hedden, T., Venkataraman, A., Evans, K. C., Lazar, S. W., & Buckner, R. L. (2010). Intrinsic functional connectivity as a tool for human connectomics: Theory, properties, and optimization. *Journal of Neurophysiology*, *103*, 297–321.
van Kesteren, M. T., Beul, S. F., Takashima, A., Henson, R. N., Ruiter, D. J., & Fernández, G. (2013). Differential roles for medial prefrontal and medial temporal cortices in schema-dependent encoding: From congruent to incongruent. *Neuropsychologia*, *51*, 2352–2359.
van Kesteren, M. T., Fernandez, G., Norris, D. G., & Hermans, E. J. (2010). Persistent schema-dependent hippocampal-neocortical connectivity during memory encoding and postencoding rest in humans. *Proceedings of the National Academy of Sciences, U.S.A.*, *107*, 7550–7555.
Vargha-Khadem, F., Gadian, D. G., Watkins, K. E., Connelly, A., Van Paesschen, W., & Mishkin, M. (1997). Differential effects of early hippocampal pathology on episodic and semantic memory. *Science*, *277*, 376–380.
Vilberg, K. L., & Rugg, M. D. (2007). Dissociation of the neural correlates of recognition memory according to familiarity, recollection, and amount of recollected information. *Neuropsychologia*, *45*, 2216–2225.
Vincent, J. L., Snyder, A. Z., Fox, M. D., Shannon, B. J., Andrews, J. R., Raichle, M. E., et al. (2006). Coherent spontaneous activity identifies a hippocampal-parietal memory network. *Journal of Neurophysiology*, *96*, 3517–3531.
Wang, S. F., Ritchey, M., Libby, L. A., & Ranganath, C. (2016). Functional connectivity based parcellation of the human medial temporal lobe. *Neurobiology of Learning and Memory*, *134*, 123–134.
Wang, J. X., Rogers, L. M., Gross, E. Z., Ryals, A. J., Dokucu, M. E., Brandstatt, K. L., et al. (2014). Memory enhancement: Targeted enhancement of cortical-hippocampal brain networks and associative memory. *Science*, *345*, 1054–1057.
Westphal, A. J., Wang, S., & Rissman, J. (2017). Episodic memory retrieval benefits from a less modular brain network organization. *Journal of Neuroscience*, *37*, 3523–3531.
Xiao, X., Dong, Q., Gao, J., Men, W., Poldrack, R. A., & Xue, G. (2017). Transformed neural pattern reinstatement during episodic memory retrieval. *Journal of Neuroscience*, *37*, 2986–2998.
Zeithamova, D., Dominick, A. L. L., & Preston, A. R. R. (2012). Hippocampal and ventral medial prefrontal activation during retrieval-mediated learning supports novel inference. *Neuron*, *75*, 168–179.
Zeithamova, D., Maddox, W. T., & Schnyer, D. M. (2008). Dissociable prototype learning systems: Evidence from brain imaging and behavior. *Journal of Neuroscience*, *28*, 13194–13201.
Zeithamova, D., & Preston, A. R. (2010). Flexible memories: Differential roles for medial temporal lobe and prefrontal cortex in cross-episode binding. *Journal of Neuroscience*, *30*, 14676–14684.
Zeithamova, D., & Preston, A. R. (2017). Temporal proximity promotes integration of overlapping events. *Journal of Cognitive Neuroscience*, *29*, 1311–1323.